Proc. Natl. Acad. Sci. USA
Vol. 96, pp. 1048–1053, February 1999
Medical Sciences

The stretch-activation response may be critical to the proper functioning of the mammalian heart

RAMESH VEMURI*, EDWARD B. LANKFORD†, KARL POETTER*‡, SHAHIN HASSANZADEH*, KAZUYO TAKEDA§, ZU-XI YU§, VICTOR J. FERRANS§, AND NEAL D. EPSTEIN*¶

*Cardiology Branch, National Heart, Lung, and Blood Institute, National Institutes of Health, Bethesda, MD 20892-1650; †Cardiovascular Section, Hospital of the University of Pennsylvania, Philadelphia, PA 19104-4283; and §Pathology Section, National Heart, Lung, and Blood Institute, National Institutes of Health, Bethesda, MD 20892-1518

Edited by Manuel F. Morales, University of the Pacific, San Francisco, CA, and approved December 3, 1998 (received for review May 1, 1998)

ABSTRACT **The "stretch-activation" response is essential to the generation of the oscillatory power required for the beating of insect wings. It has been conjectured but not previously shown that a stretch-activation response contributes to the performance of a beating heart. Here, we generated transgenic mice that express a human mutant myosin essential light chain derived from a family with an inherited cardiac hypertrophy. These mice faithfully replicate the cardiac disease of the patients with this mutant allele. They provide the opportunity to study the stretch-activation response before the hearts are distorted by the hypertrophic process. Studies disclose a mismatch between the physiologic heart rate and resonant frequency of the cardiac papillary muscles expressing the mutant essential light chain. This discordance reduces oscillatory power at frequencies that correspond to physiologic heart-rates and is followed by subsequent hypertrophy. It appears, therefore, that the stretch-activation response, first described in insect flight muscle, may play a role in the mammalian heart, and its further study may suggest a new way to modulate human cardiac function.**

The human heart is a prodigious organ that beats ≈3 billion times during a 70-year lifetime. It is powered by the cardiac isoform of the myosin molecule, a molecular motor that transduces chemical energy released by its ATPase activity into directed movement. This myosin molecule has a globular head tapering to a slender neck to which two myosin light chains are bound. The neck is connected to a rod-like tail that is responsible for the self assembly of myosin molecules into thick filaments. In striated muscle, actin-containing thin filaments are moved past interdigitating thick filaments by myosin heads, which extend from the thick filaments and asynchronously deliver repetitive impulses to actin (1–3). The interdigitating filaments are arranged in a quasicrystalline lattice geometry that influences the strain between actin and myosin molecules in the fiber. Because individual myosin heads are constrained by this lattice organization, a series elastic element must store mechanical energy to accommodate the asynchronous crossbridge action. Variations in myosin isoforms, associated proteins, and lattice spacing introduce diversity in actomyosin interaction and power output of the muscle fiber (4, 5).

Insect flight muscle (IFM) has evolved to accentuate and exploit a property that is of unknown physiologic significance in other types of muscle fibers. The wing beat frequency of the common fly is ≈150 beats/s. It would be energetically very costly to repetitively pump calcium ions across the sarcoplasmic membrane at this rate. Instead, an exaggerated stretch-activated response (active in the presence of a constantly elevated calcium level) generates oscillatory power output in IFM. This stretch-activation response was first described in Pringle's studies of IFM in 1949 (6). More recently, Kawai refers to it as "process B" and routinely observes it in sinusoidal oscillation studies of heart and skeletal muscle fibers (7, 8). The stretch-activation response is manifested as a "delayed tension" when an activated muscle fiber is subjected to a quick stretch or release. This phenomenon is appreciated in a plot of tension vs. time after a quick stretch of activated muscle. After stretch, there is an immediate proportional elastic increase in tension followed by quick decay. Then there is a second rise in tension, even though the muscle fiber remains isometric (9) (normal fiber in Fig. 2). This second rise in tension is a delayed response that follows the length change and is the signature of a stretch-activation response (10). The time delay of this second rise in tension is related to the resonant frequency of maximal power output in an oscillating system. In IFM, the delay is ≈50 ms (11); in rabbit heart papillary muscle it is ≈1.2 s (11). The heart muscle is stimulated by electrically activated calcium transients. However, the extent to which an intrinsic myogenic stretch-activation response is matched to heart rate may augment the oscillatory power of cardiac myofibers (9).

Recently, mutations in the human essential light chain (ELC) and the regulatory light chain (RLC) associated with the inherited midventricular cavity obstruction phenotype of hypertrophic cardiomyopathy were described (12). It was speculated that the rare cardiac papillary muscle hypertrophy, associated with mutations in either myosin light chain, reflected a common effect on myosin function because of changes in the neck region of the myosin molecule. These mutations may disrupt the stretch-activation response of the cardiac papillary muscles and adjacent ventricular tissue through a change that they produce in the elasticity of the neck region of the myosin molecule. The change in stretch-activation, resulting from these molecular defects, presumably reduces the oscillatory power of the papillary muscles, normally augmented by the stretch-activation response. Over time, this leads to a compensatory hypertrophic response that increases power but eventually obstructs the ventricular cavity. To test this hypothesis, we constructed transgenic mice expressing either the normal or the mutant human ELC from an affected family with midventricular cavity hypertrophic cardiomyopathy and examined the effect on disease progression and the stretch-activation response.

MATERIALS AND METHODS

Generation of Transgenic Mouse Lines. A 12-kilobase fragment containing ≈5 kilobases of promoter region, all seven exons, and the intervening introns together with 1.3 kilobases of 3′ sequence was cloned from a human cosmid library (12). A single nucleotide change producing the $149^{\text{Methionine}\rightarrow\text{Valine}}$ mutation was introduced. The mutant human and the control human constructs were resequenced and then were used to produce

The publication costs of this article were defrayed in part by page charge payment. This article must therefore be hereby marked "*advertisement*" in accordance with 18 U.S.C. §1734 solely to indicate this fact.

PNAS is available online at www.pnas.org.

This paper was submitted directly (Track II) to the *Proceedings* office.
Abbreviations: ELC, essential light chain; RLC, regulatory light chain; IFM, insect flight muscle.
‡Present address: Austin Research Institute, Studley Road, Heidelberg, VIC 3084, Australia.
¶To whom reprint requests should be addressed. e-mail: nepstein@helix.nih.gov.

transgenic mice as described (13). Ten founder mice expressing the human $149^{\text{Methionine}\rightarrow\text{Valine}}$ mutant allele of the ELC and six founder mice with the control human allele of the ELC were obtained. Lines from all 16 founders were developed by breeding each founder separately into C57B/J6 hybrid mice. These lines have been continued for 2 years. Animal care has been in accordance with Animal Care and Use Committee guidelines as stated in protocol 5-CB-7.

Generation of Antibody to Mutant ELC. Mutant peptide (CNGTV**V**GA) was affixed to Sepharose 4B (Pharmacia) via free amines and was used to affinity-purify the rabbit antisera produced against the mutant peptide. The column was washed and eluted in low pH glycine. Eluant was cross-absorbed against the wild-type peptide (CNGTV**M**GA).

Analysis of Papillary Muscles. Mice were killed, and the hearts were rapidly excised. The right ventricles were opened, and the papillary muscles were excised and pinned into a dish containing a high EGTA permeabilizing solution (14) maintained at 2°C. After 4 hours, the solution was replaced by one containing 50% glycerol and was kept at −20°C.

Measurement Apparatus. Each muscle strip examined was mounted between a silicon strain gauge force transducer and a servo motor in a temperature-controlled chamber at 20°C, with a low calcium concentration (relaxing) solution. The system has a force transducer element (Akers, Horten, Norway) with custom mounting, which has a natural resonance at 5.6 kHz but, with damping, has a flat frequency response up to 3 kHz. The frequency response of the servo motor (6350; Cambridge Technology, Cambridge, MA) is limited by a resonance at 1300 Hz. Control of muscle length was performed by using custom software written in our laboratory. The software controlled a programmable filter (9002; Frequency Devices, Haverhill, MA) and a digital oscilloscope (model 54600A; Hewlett–Packard). Data consisting of force and motor position (hence muscle length) were sampled by using an A/D board (DT2828; Data Translation, Marlboro, MA) with 12 bits of resolution at a frequency of 5 kHz for the quick stretch experiments. For dynamic stiffness measurements, the sampling frequency varied from 16 kHz at the high driving frequencies down to 40 Hz at a driving frequency of 0.02 Hz. The programmable filter (8 pole Bessel with linear phase) was set to low pass filter at a frequency 1/8 (at high frequencies) to 1/64 (at lower frequencies) of the data acquisition rate to avoid aliasing. Data were collected over 256 sinusoidal cycles at 500 Hz and over 1 cycle at 0.02 Hz. Stabilization sinusoidal driving was performed at each frequency for ≈0.5 s, during which time data was not saved. Data were saved on an 80486 computer and were analyzed off-line by using our custom software.

Muscle Protocol. The muscle fibers were mounted and stretched in relaxing solution to ≈110% of slack length. Muscle dimensions were measured optically under a dissecting microscope. Under computer control, the servo motor was driven sinusoidally at 55 selected frequencies from 500 Hz to 0.02 Hz. The length changes chosen were 0.1% muscle length, but amplitudes between 0.05 and 0.5% gave similar results. The sinusoidal amplitude of 0.1% was as small as technically feasible to minimize the nonlinearities of viscoelastic tissues. The signals representing motor position (muscle fiber length) and force were digitized and recorded to computer disk. Then, the bathing solution was changed briefly to a "preactivating solution" similar to the relaxing solution but with 20 mM 1,6-hexamethylenediamine-*N*,*N*,*N*′,*N*′-tetraacetic acid replacing the EGTA. It then was changed to a high calcium solution of the following composition, in mM: Na 51, K 86, Cl 13, PCr 20[‖], EGTA 25, N-Tris[hydroxymethyl]methyl-2-aminoethanesulfonic acid 100, MgATP 5, reduced glutathione 10, leupeptin 0.1, and sufficient CaEGTA to obtain a pCa of 4.3. After steady isometric force was reached, the muscle was step-wise stretched to 1% of its initial length, and the force signal was recorded for 4 s. Then, the motor again was driven at each of 55 discrete frequencies between 500 Hz and 0.02 Hz, and the motor position and force signals were recorded. The bathing solution was replaced with an identical solution without any ATP or creatine phosphate with a flow-through wash of >5× the chamber volume. The dynamic stiffness again was determined in this rigor solution.

Data analysis included determining the isometric force before any stretches, displaying the force levels during the 1% step-wise stretch, and measuring the time-to-peak of the delayed force, the amplitude of the delayed force, and the force amplitude for 4 s of stretch. Initial isometric force was normalized to cross-sectional area to give stress (kN/m^2). To compare the quick stretch experimental data, forces during these stretches were normalized to initial isometric prestretch force. During the experiments in which the fiber bundles were sinusoidally lengthened and shortened, the signals representing the changing fiber length and the force were collected for each of the discrete frequencies.

The fast Fourier transform was used on the length signal to determine the driving frequency of the length oscillation, and its amplitude and phase. At this driving frequency, the fast Fourier transform of the force signal was computed to determine the force oscillation amplitude and phase. The response of the fibers was computed as the ratio of the force amplitude to length amplitude (modulus, or stiffness) and the force phase minus the length phase. The impedance at each frequency consists of both the magnitude ratio and phase. These transforms were computed at each frequency for each condition (relaxed, activated, and rigor). Thus, correction for the fiber response to series viscoelasticities (measured as end-compliance) was accomplished through analysis of rigor fibers preloaded to the tension of the activated fiber. Parallel viscoelasticities were determined in fibers under relaxed conditions and were subtracted from the activated response.

Fiber dimensions and isometric force values were compared by using SIGMA-STAT for Windows (SPSS, Chicago) Comparisons were made by using a one-way ANOVA, and if a test of sample normality was not met, a Kruskal-Wallis one-way ANOVA on Ranks was performed. Statistical significance was set at $P < 0.05$, and deviations are reported as mean ± SD.

RESULTS AND DISCUSSION

Because hypertrophic cardiomyopathy is an autosomal dominant disease (15), the mutant gene expressed in parallel with the normal homologous gene causes disease. Thus, in these transgenic mice, the mutant or normal human ELC gene was added to a normal mouse background. The entire human cardiac ELC gene with its own promoter was used to create transgenic mouse lines expressing either the human control or the human mutant $149^{\text{Methionine}\rightarrow\text{Valine}}$ ELC. This promoter is active in both heart and slow skeletal muscle. Six founder transgenic mice expressing the control human ELC and 10 founder mice expressing the mutant human ELC were produced. Reverse transcription–PCR and sequencing demonstrated proper splicing and expression of the control human and mutant human message in both the heart and slow skeletal muscle of the transgenic lines (data not shown). An antibody to seven amino acids, incorporating the $149^{\text{Methionine}\rightarrow\text{Valine}}$ substitution, three residues from the carboxy-terminal end of the peptide, was raised in rabbits and was cross-absorbed against the wild-type peptide. This antibody reacted strongly with the mutant human ELC but not with the endogenous mouse ELC in fresh frozen sections from normal mice (Fig. 1 *G–I*). However, the antibody did not distinguish between the mutant and endogenous protein under the denaturing conditions of a Western blot. Nonetheless, in tissue sections, the antibody demonstrated that the mutant human ELC was

[‖]Although we are aware that that absence of exogenous creatine kinase and 20 mM PCr place our regenerator capacity in a low range, we feel that it is nevertheless adequate at 20°C and permits a legitimate comparison of control and experimental fibers.

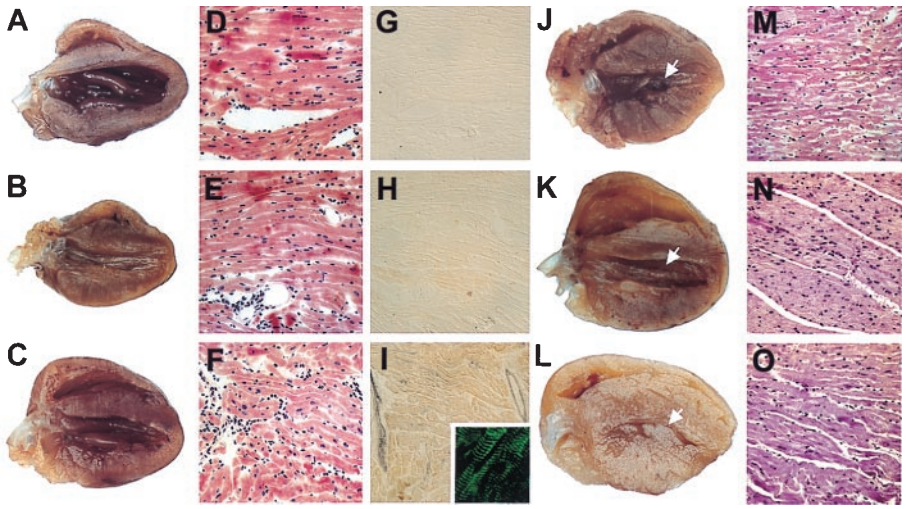

FIG. 1. Representative gross anatomy, histology, and immunohistology of normal mouse hearts compared with hearts from transgenic mice expressing the normal human ELC (human control) or mutant human ELC (mutant human) at 3 months and at 1 year of age. (*A–C*) Hearts from normal (*A*), human control (*B*), and human mutant (*C*) mice, respectively, at 3 months of age are similar. (*D–F*) The morphology in H- & E-stained sections of the three hearts shown in *A–C* is normal. (×50.) (*G–I*) Immunoreactivity after staining with polyclonal antibody against mutant ELC is absent in normal hearts (*G*), minimal in human control hearts (*H*), and strong in the human mutant hearts (*I*) HR peroxidase method was used. (×50.) (*I*, *Inset*) Localization of reactivity in myofibrills by using a fluorescein isothiocyanate-conjugated (green) secondary antibody. (×150.) (*J–L*) Hearts from three different normal (*J*), human control (*K*), and human mutant (*L*) mice at 1 year. Solid arrows in *J* and *K* show normal left ventricular cavity. Arrow in *L* shows hypertrophied papillary muscle obstructing the middle of the mostly obliterated left ventricular cavity. (*M–O*) H- and E-stained sections of normal (*M*), human control (*N*), and human mutant (*O*) hearts at 1 year. *M* and *N* are normal; *O* shows myocyte hypertrophy without disarray. (×50.)

uniformly and properly incorporated into the sarcomeres throughout the mutant human mouse hearts (Fig. 1 *I* and *I*, *Inset*).

At 3–5 months of age, the gross morphology and histology of both the mutant human and human control mice were indistinguishable from those of normal mice (Fig. 1 *A–C*). The right ventricular papillary muscle bundles from these three groups of mice were studied with respect to (*i*) isometric tension development, (*ii*) the time delay to the second rise in tension in quick stretch experiments, and (*iii*) the tension response to sinusoidal length modulations of the muscles at discrete frequencies ranging from 0.02 to 500 Hz.

The isometric tension of seven normal mouse, eight control human mouse, and nine mutant human mouse papillary muscles first was evaluated. The irregular conical shape of the papillary muscles introduces a degree of uncertainty into measurements of stress (tension/mm^2) caused by the imprecise denominator. With this caveat, however, bundle cross-section was taken to be represented by the transverse dimension at the "shoulder" of the muscle bundle, where it tapers sharply toward the tendonae to an apical diameter of approximately one-third to one-half of the measured shoulder dimension. The measurements at the shoulder were 0.070 ± 0.041, 0.057 ± 0.028, and 0.051 ± 0.027 mm^2 for the normal, control human, and mutant human mice, respectively ($P = 0.42$). The corresponding measurements of tension were 0.53 ± 0.28, 0.26 ± 0.16, and 0.34 ± 0.24 mN ($P = 0.06$). Normalizing tension by cross section gave the corresponding values for stress of 9.2 ± 1.8, 5.2 ± 0.6, and 8.3 ± 2.1 kN/m^2 ($P = 0.21$ using ANOVA on ranks), demonstrating no significant difference between the normal and mutant human papillary muscles with respect to normalized tension development.

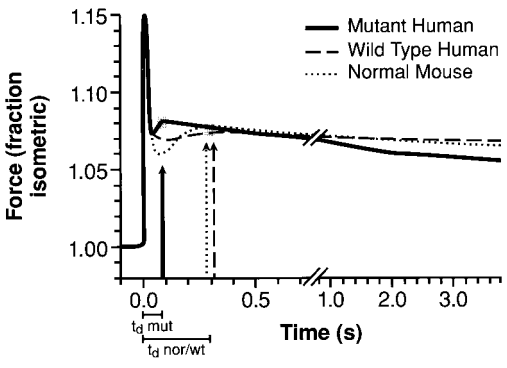

FIG. 2. Tension as a function of time after a step increase of 1% in length of right ventricular papillary muscles from 3- to 4-month-old mice. The average of tension transients from muscles of three normal mice (normal), three transgenic mice expressing the normal human ELC (human control), and four transgenic mice expressing the mutant human ELC (human mutant) are as noted in the key. Three- to four-month-old mice were used to avoid hypertrophy in the human mutant mice. The corresponding vertical arrows in each case mark the peak of the "second rise in tension." Just below the time axis are shown the corresponding time delays (t_ds) with time origin at 0 s from the initiation of stretch. The three traces show that the t_d for the muscles from the human mutant mice is ≈1/3 that for the normal and human control mice.

The averaged stretch-activation responses of right ventricular papillary muscle bundles from normal, control human, and mutant human 3- to 4-month-old mice are shown in Fig. 2. The normalized tension transients of papillary muscles from four normal and four control human mice are of similar form. A time delay to the second rise in tension of 255 ± 96 and 258 ± 60 ms is present in the two respective groups. In contrast, the transients of papillary muscles from six mutant human mice have a time delay to the second rise in tension of 107 ± 29 ms. The data from the individual experiments were approximated to exponentials and were extrapolated to zero to obtain measures of $t_{1/2}$ to facilitate the following analysis similar to Steiger's (11). The values, with the SEM, are 67.5 ± 22.5, 71.25 ± 17.4, and 24.7 ± 3.9 ms for the normal, control human, and mutant human mice, respectively. Apparent rate constants (r) can be estimated from the exponentials by dividing the half-times into 0.69. These are: 10.2 ± 3.4, 9.7 ± 2.4, and 27.9 ± 4.4 s^{-1}, respectively. The rate constants (r) can be converted to frequency (f) of maximum power output/cycle by using the relation $r = 2\pi f$ (7, 8, 11).

The quick stretch experiments were performed at 20°C, which is below physiologic temperature, to preserve fiber integrity. Rates can be adjusted to a physiologic temperature of 40°C by using a factor (Q_{10}) of 3 per 10°C change as reported (9, 11, 16, 17). With this adjustment, the maximum frequency (f) of power output/cycle of the muscle bundles lies in the range of 876 and 834 cycles/min in the normal and control human mice, respectively (within the range of the normal mouse heart rate**). In contrast, the frequency of maximal power-output/cycle for the mutant human mouse muscle bundles lies in the range of 2,124 cycles/min, much faster than the heart rate of the mouse. Thus, despite the similar normalized isometric tension production by normal and mutant mice, the increased oscillatory power output

**We have observed the heart rate of anaesthetized mice between 435 and 560 beats/min. Heart-rate increases in active mice (N.D.E., unpublished observation).

that can come from the stretch-activation response will not be available in the mice expressing the mutant human ELC. On the other hand, increased oscillatory power from the stretch-activation response is available to the hearts of both the normal and control human mice within the physiologic range of the heart rate.

The quick-stretch experiments are subject to uncertainties in normalized tension measurements and are further complicated by the fact that papillary muscles may vary in the amounts of connective tissue from base to tip. However, in contrast to the normalized tension amplitudes of the quick-stretch experiments, the resonant frequency of muscle bundles is independent of bundle thickness. Furthermore, the possible confounding effect of variation in the amount of connective tissue can be minimized by correcting the response of activated muscle bundles by the response of relaxed and rigor muscle bundles. This makes the determination of resonant frequency a reliable way to compare the muscle bundles from the three groups of mice.

The resonant frequency at which power is absorbed and then released by a muscle bundle is determined by the time delay to the second rise in tension measured in the quick-stretch experiments. This relationship can be visualized by considering a muscle fiber that is repetitively lengthened and then shortened by an apparatus that sinusoidally modulates the length of the fiber. As the fiber is stretched, the immediate (in phase) increase in tension that is recorded is purely elastic and is followed by an expected drop in tension, presumably as crossbridges detach. This drop in tension, in turn, is followed by the second rise in tension characteristic of the stretch-activation response. The time after the stretch until the peak of the second rise in tension determines the frequency at which work absorbed during stretch is exceeded by work delivered during shortening, producing net work on the driving apparatus.

A plot of tension vs. length (or stress vs. strain) during such sinusoidal oscillations is ellipsoid with a counter-clockwise direction, indicating that tension at the same fiber length is greater during the shortening portion of the cycle than during the lengthening portion of the cycle. As frequency is changed, the work loop closes and reverses direction to become clockwise. With the reversal in direction of the work loop, the shortening fiber no longer produces work on but, rather, absorbs work from the driving apparatus. We record the frequency at which the work loop changes direction (at which phase passes through zero) as a marker frequency that helps characterizes the dynamic contractile properties of the muscle bundle. The integrated area of the loop gives a measure of the work performed or absorbed. When a stress vs. strain plot traces a line (zero phase shift) rather than a loop, no work is produced during the cycle and the relationship of tension to length is purely elastic.

Fig. 3 depicts the work loops obtained in a plot of stress vs. strain of papillary muscle bundles from a representative normal, control human, and mutant human mouse. These studies, performed at frequencies of 5.0, 1.0, and 0.3 Hz, at 20°C, require adjustment by a Q_{10} of 3, as used above, to determine the range of the corresponding heart rates. This adjustment yields values of 2,700, 540, and 160 beats/min, respectively. The bottom panel of Fig. 3. depicts the work loops at 0.3 Hz. The papillary muscles from all three groups show a counter-clockwise direction, with a net production of work on the driving apparatus. At this frequency, however, the mutant human mouse loop is so narrow as to hardly produce any work at all. At 1.0 Hz, shown in the middle panel of Fig. 3, the papillary muscle from both the normal mouse and the control human mouse have a clockwise direction and absorb work from the driving apparatus during the shortening portion of the cycle. In contrast, the papillary muscles from the mutant human mouse continues to have a counter-clockwise direction, and the increased area circumscribed by this loop signifies that some work is performed on the apparatus by the muscle bundle during shortening. In the top panel of Fig. 3, at 5.0 Hz, all three groups of muscle bundles absorb work during oscillation. In these experiments, the frequency of phase shift of the mutant human mouse is skewed to the higher frequencies compared with the normal and control human mouse. This is consistent with the shorter time to the second rise in tension observed in the quick-stretch experiments on the mutant human mouse papillary muscle.

The work loops in Fig. 3 are for one representative papillary muscle from each of the three groups. To evaluate the average phase shift for each of the groups, the stress–strain data, corrected for the relaxed and rigor response, was averaged for each of the three groups of mice. The corresponding phase shifts associated with the fast Fourier transforms of the averaged files from normal, control human, and mutant human mouse papillary muscles were determined by correcting for relaxed and rigor response. This yielded the phase shift for the average of three papillary muscles from each of the three groups of mice and is shown in the Bode phase plot depicted in the upper panel of Fig. 4. The phase shift is plotted against frequency of oscillations. A negative phase corresponds to a counter-clockwise direction of a work loop. Mutant human mouse muscle bundles show a negative phase between 0.9 and 2.6 Hz, in contrast to the normal mouse preparations, which are negative in phase between 0.3 and 0.5 Hz. Control human mouse muscle bundles show a negative phase at

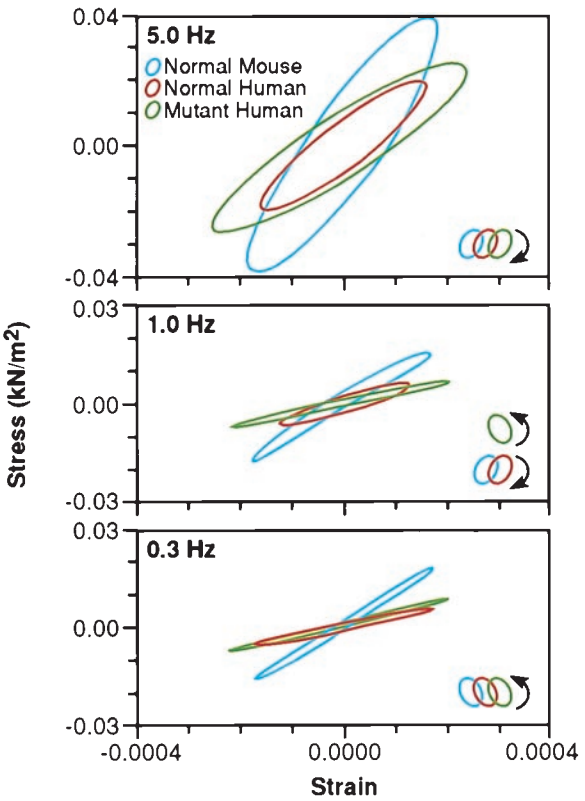

FIG. 3. Smoothed work loops from raw data of fiber stress versus strain (normalized tension vs. fractional change in length) during sinusoidal length oscillations of representative normal, control human, and mutant mouse papillary muscles at three frequencies. Raw saved data was digitally filtered at 16× the driving frequency to reduce electrical noise (primarily 60 Hz). Data is shown at each frequency for the three types of muscle bundles. The muscle bundle type and direction of the work loop are identified by color and arrows respectively, in the legend. In the top panel are loops during 5.0 Hz oscillations showing that, at this frequency, all muscle bundles absorb work from the driving apparatus. The clockwise rotation of the loops indicates that, during shortening, the force exerted is lower than during lengthening. In the middle panel, at 1.0 Hz, only the mutant human bundle performs work on the driving apparatus, as indicated by the counter-clockwise rotation. In the bottom panel, at 0.3 Hz, all three bundles traverse a counter-clockwise loop, indicating the production of work, although the mutant loop is so narrow as to hardly produce any work at all.

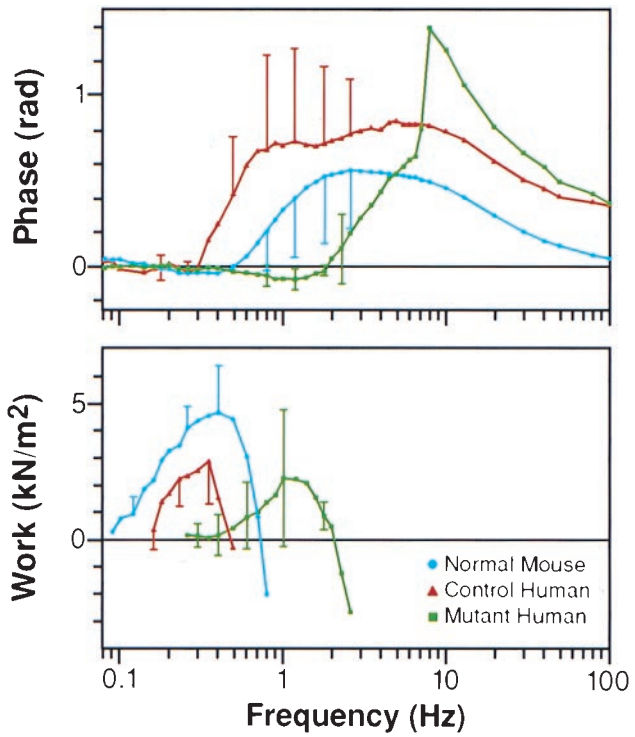

FIG. 4. Composite Bode plot showing the response of papillary muscle (three muscles of each type) to oscillations over the frequency range of 0.08–100 Hz. The upper panel shows that the phase becomes negative in human mutant mice (force lags length, indicating work producing) between frequencies of 0.9 and 2.6 Hz. The normal mouse papillary muscles have negative phase between frequencies of 0.3 and 0.5 Hz, with error bars too small to show. Human control mouse papillary muscles have a negative phase below frequencies of the normal mouse. The lower panel shows the mean calculated work per loop for the three muscle types. The peak work/cycle is produced between 0.3 and 0.4 Hz in the normal and control human muscle bundles. Work at this frequency is minimal in the mutant muscle bundles in which the peak work/cycle has been shifted to ≈1.3 Hz.

frequencies even lower than the normal mouse. The lower panel shows the average calculated work per cycle vs. frequency. The frequency of peak power output is shifted to the higher frequencies in the mutant muscle bundles compared with normal and control human mouse controls. The normal human control mice in both plots confirm that this shift is not the result of inappropriate expression of human ELC in mouse heart.

The resonant frequencies calculated for the three groups of mice from the quick-stretch experiments are higher than those predicted by the frequency range of negative phase in the Bode plots. This is not surprising because the quick-stretch experiments involve a 1.0% of muscle length stretch and the sinusoidal oscillations use a 0.1% stretch. The kinetics will differ significantly between both systems, but both types of length modulations show a dramatic upward shift of the resonant frequencies of the mutant human mouse preparations out of the range of the physiologic mouse heart rate. Such an increase in the apparent rate constant of the stretch-activation response could theoretically be the result of increased inorganic phosphate (7, 8) that fails to diffuse out of the mutant human muscle bundle. However, the inorganic phosphate effect described by Kawai (7, 8) is mostly limited to the middle frequency range, with a minimal effect in the lower and higher frequency range, unlike the alterations in phase shift seen in these mutant human mouse muscle bundles (Fig. 4 *Upper*).

The upward shift in resonant frequency suggests a change in crossbridge recruitment. Changes in crossbridge cycling also have been observed with altered light chains in myosin *in vitro* motility assays as well as in fiber studies of unloaded velocity with substituted light chains (12, 18–20). The increased unloaded velocity is presumably attributable to a strain-dependent increased rate of crossbridge detachment. An increased rate of detachment could shorten the duty cycle and diminish internal resistance. This could lead to the observed increase in unloaded velocity (12) in the context of diminished force (Fig. 4 *Lower*). An increased rate of head detachment would increase the number of dissociated heads, increase the apparent rate constant of attachment, and accelerate the stretch-activation response.

The experiments described above all were performed on the three groups of mice at 3–4 months of age, when there is no gross pathologic or histologic changes. This age restriction was maintained to remove any confounding secondary effects that might be attributable to hypertrophy. By 1 year, hearts from normal as well as all six control human mouse lines continue to show normal histology and gross morphology of the ventricular cavities. In contrast, there is hypertrophy of the papillary muscles and the adjacent ventricular tissue in all 10 mutant human independent founder mice and their progeny. Such a robust finding virtually excludes the possibility that the effect of the mutant ELC is an idiosyncrasy of transgene insertion sites (Fig. 5).

The unique morphology of midcavity hypertrophy in the mice with a distortion of the stretch-activation response highlights portions of the heart that are likely to normally exploit this intrinsic myogenic property. In contrast, although the mutant ELC is expressed in the slow skeletal muscle of the mutant human mice, there is no evidence of hypertrophy, by gross or histologic examination, in the soleus muscles of these mice at any age. This suggests a minor or, at least, different physiologic importance of the stretch-activation response in skeletal muscle. The papillary muscles tether the atrioventricular valves during the ventricular contracting portion of the cardiac cycle, thus preventing backflow of blood into the atrium. However, it is likely that they contribute to cardiac function in other ways because their removal (once common in the course of surgical replacement of the mitral valve) leads to cardiac failure (21).

The papillary muscles are the only ventricular cardiac fibers that exert a direct unidirectional pull between their origin and their site of attachment (22). In this way, and in their prominent stretch-activation property and oscillatory power-output, they resemble IFM. It is likely that distortion of the stretch-activation response of papillary muscle in the mutant mice leads to an

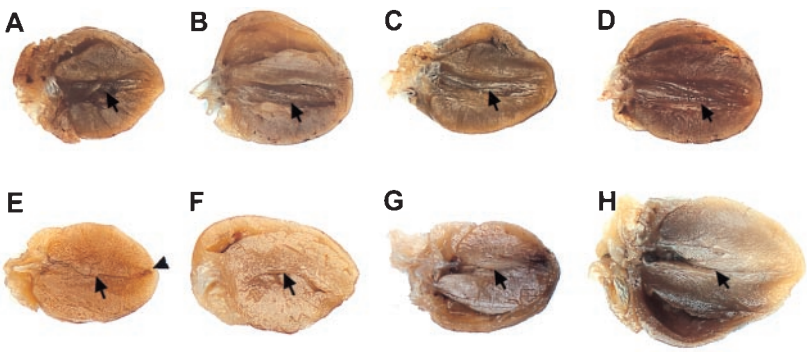

FIG. 5. Comparison of adult transgenic mouse hearts to a normal adult mouse heart. At 1–1.5 years of age, gross cardiac morphology is normal in normal mouse (*A*) and in hearts from three independent transgenic human control mouse lines (*B–D*); arrows show normal left ventricular cavity. However, the hearts from four independent transgenic mutant human transgenic mouse lines (*E–H*) show a thin apex (arrowhead) and obliteration of the middle of the left ventricular cavity (arrows).

inadequate performance, which, in turn, maintains a stimulus for hypertrophy. The adjacent myocardium at the base of the papillary muscles also hypertrophies for unclear reasons. Perhaps the stretch-activation response is also important there, despite its more complex myofiber architecture. Alternatively, the periodic stretch and contraction of papillary muscles may aid force development of the adjacent deeper fibers at the base of the papillary muscles. Another possibility is that the signal to hypertrophy coming from subnormally functioning papillary muscle "spills over" to the adjacent ventricular tissue.

The wave of mechanical activation that spreads throughout the heart begins at its inner surface, which includes the trabeculae carnae and papillary muscles (22). During the isovolumic portion of contraction, the papillary muscles contract to keep the atrioventricular valves from everting into the atrium. As the ventricles contract during "isovolumic contraction," there is some slight change of chamber shape, and some blood in the ventricles begins to move toward the atria. This exerts a tug on the papillary muscles at the same time that the majority of the ventricular myofibrils are shortening. The papillary muscles must continue to exert tension during all of systole, during which time the wave of electrical activation has moved on to the deeper ventricular tissues. Therefore, papillary muscle function probably benefits from an increased amplitude and duration of tension production. We believe that this increased amplitude and duration of tension could be supplemented by the delayed tension produced in stretch-activated fibers.

The three-dimensional structure of myosin (23–25) shows that the myosin neck is mostly formed by a long α-helix that is reinforced by the two light chains, the ELC being proximal to the distal RLC. These light chains may act as cervical collars that stabilize the neck. Evidence exists to support the idea that they affect the rigidity or stiffness of the neck (26), which, consequently, may act as a rigid lever, amplifying and transmitting small movements of the globular head to produce an appropriate stepsize. There is evidence for movement of the neck region of some myosin isoforms during the cross-bridge cycle (27–28). Other studies have shown that loss of the ELC, substituted light chains, or changes in neck length can affect *in vitro* assays of unloaded duty cycle or velocity (29–31).

We previously speculated that naturally occurring mutations in either the myosin ELC or RLC distorted a stretch-activation response that is critical to myofibers in certain portions of the heart (12). This could occur through an alteration in the stiffness or elasticity of the neck region, which, in turn, could influence strain-dependent rate constants that govern the cyclic attachment and detachment of crossbridges. Changes to this cycle could interfere with timing and distort oscillatory power in the way that faulty timing affects power of an automobile engine.

The three mutations in the RLC of patients that we reported earlier (12) surround a phosphorylatable serine that is critical to smooth and nonmuscle myosin function but only has been observed to be modulatory in striated muscle myosin at submaximal levels of activation (32–34). The mutations that surround the phosphorylatable serine could affect flexibility of the myosin neck region independently and/or through the efficiency of phosphorylation. Some patients with these RLC mutations surrounding this serine have the same rare midcavity phenotype (characterized by pronounced papillary muscle hypertrophy) as the patients (12) and the transgenic mice expressing the patients mutant ELC. This rare phenotype, at the present time uniquely associated with mutations in either light chain, led to our speculation that the RLC mutations in patients also could lead to a distortion of the stretch-activation response through a regional effect on the neck of the myosin molecule.

This speculation is consistent with the observed loss of stretch-activation, decreased oscillatory power output, and the consequent flightlessness of transgenic *Drosophila* missing the homologous serines in the RLC (35). In these transgenic *Drosophila*, however, the loss of stretch-activation was not associated with a change in rate of cross-bridge cycling but, rather, of magnitude. This contrasts with the change in rate of crossbridge cycling evident in the mutant human mouse presented here. However, either a decreased magnitude of stretch-activation or a shift of the response to beyond the physiologic range should have the similar consequence of decreased oscillatory power in the organism.

Our observations lead to an intriguing possibility that variations in the level of RLC phosphorylation may modulate the stretch-activation response by "retuning" the myosin motors and consequently the resonant frequency of the myofibers. This would provide a mechanism by which cardiac myosin power output/cycle normally could be adjusted to match a faster rate of contraction and relaxation during extended periods of increased heart rate. This possible mechanism presently is being tested in our laboratory with novel transgenic mice. If this pathway is shown to alter cardiac efficiency, then pharmaceutical modulation of cardiac RLC phosphorylation may provide a new route to therapeutic interventions in heart failure from a variety of causes.

We thank Ms. Kim Daniels for excellent technical assistance and Dr. J. S. Davis for help with curve fitting and careful reading of the manuscript. The transgenic mice were generated under National Institute of Child Health and Human Development Contract 1-HD-5-3229. E.B.L. is supported in part by Southeastern Pennsylvania Affiliate of the American Heart Association Grant-in-Aid and National Institutes of Health Grant K08HL03172.

1. Huxley, A. F. (1957) *Prog. Biophys. Biophys. Chem.* **7,** 225–318.
2. Huxley, H. E. (1969) *Science* **164,** 1356–1366.
3. Huxley, A. F. & Simmons, R. M. (1972) *Nature (London)* **233,** 533–538.
4. Swynghedauw, B. (1986) *Physiol. Rev.* **66,** 710–771.
5. McDonald, K. S. & Moss, R. L. (1995) *Circ. Res.* **77,** 199–205.
6. Pringle, J. W. S (1949) *J. Physiol. (London)* **108,** 226–233.
7. Kawai, M., Sakei, Y. & Zhao, Y. (1993) *Circ. Res.* **73,** 35–50.
8. Kawai, M. J. (1986) *J. Muscle Res. Cell Motil.* **7,** 421–434.
9. Pringle, J. W. S. (1978) *Proc. R. Soc. London Ser. B* **201,** 107–130.
10. Peckham, M., Molloy, J. E., Sparrow, J. C. & White, D. C. S. (1990) *J. Muscle Res. Cell Motil.* **11,** 203–215.
11. Steiger, G. J. (1977) in *Insect Flight Muscle*, ed. Tregear, R. T. (North–Holland, Amsterdam), pp. 221–268.
12. Poetter, K., Jiang, H., Hassanzadeh, S., Master, S. R., Chang, A., Dalakas, M. C., Rayment, I., Sellers, J. R., Fananapazir, L. & Epstein, N. D. (1996) *Nat. Genet.* **13,** 63–69.
13. Pinkert, C. A. (1994) *Transgenic Animal Technology: A Laboratory Handbook* (Academic, San Diego).
14. Eastwood, A. B., Wood, K. S., Bock, K. L. & Sorenson, M. M. (1979) *Tissue Cell* **11,** 553–566.
15. Fananapazir, L. & Epstein, N. D. (1994) *Circulation* **89,** 22–32.
16. Zhao, Y. & Kawai M. (1994) *Biophys. J.* **67,** 1655–1668.
17. Davis, J. S. & Rodgers, M. E. (1995) *Biophys. J.* **68,** 2032–2040.
18. Lowey, S., Waller, S. G. & Trybus, M. K. (1993) *J. Biol. Chem.* **268,** 20414–20418.
19. Sweeney, H. L. (1995) *Biophys. J.* **68,** Suppl. 4, 112s–119s.
20. Morano, M., Zacharzowski, U., Maier, M., Lange, P. E., Alexi-Meskishvili, V., Haase, H. & Morano, I. (1996) *J. Clin. Invest.* **98,** 467–473.
21. Lillehi, C. W., Levy, M. J. & Bonnabeau, R. C. (1964) *J. Thorac. Cardiovas. Surg.* **7,** 532–543.
22. Rushmer, R. F. (1956) *Am. J. Physiol.* **184,** 188–194.
23. Rayment, I., Rypniewski, W. R., Schmidt-Base, K., Smith, R., Tomchick, D. R., Benning, M. M., Winkelmann, D. A., Wesenberg, G. & Holden, H. M. (1993) *Science* **261,** 50–58.
24. Xie, X., Harrison, D. H., Schlichting, I., Sweet, R. M., Kalakobis, V. N., Szent-Gyorgyi, A. G. & Cohen, C. (1994) *Nature (London)* **368,** 306–312.
25. Houdusse, A. & Cohen, C. (1996) *Structure* **4,** 21–32.
26. Eden, D. & Highsmith, S. (1995) *Biophys. J.* **68,** Suppl., 372s–373s.
27. Whittaker, M., Kubalek, W. E. M., Smith, J. E., Faust, L., Milligan, R. A. & Sweeney, H. L. (1995) *Nature (London)* **378,** 748–751.
28. Irving, M., Allen, T. S. C., David, S. C., Brandenmeier, B. K., Jones, K. J., Corrie, J. E. T., Trentham, D. R. & Goldman, Y. E. (1995) *Nature (London)* **375,** 688–691.
29. VanBuren, P., Waller, G. S., Harris, D. E., Trybus, K. M., Warshaw, D. M. & Lowey, S. (1994) *Proc. Natl. Acad. Sci. USA* **91,** 12403–12407.
30. Lowey, S., Waller, G. S. & Trybus, K. M., (1993) *Nature (London)* **365,** 454–456.
31. Uyeda, T. Q. P., Abramson, P. D. & Spudich, J. A. (1996) *Proc. Natl. Acad. Sci. USA* **93,** 4459–4464.
32. Sweeney, H. L. & Stull, J. T. (1986) *Am. J. Physiol.* **250,** C657–C660.
33. Morano, I. & Ruegg, J. C. (1986) *Basic Res. Cardiol.* **81,** Suppl. 1, 17s–23s.
34. Metzger, J. M., Greaser, M. L. & Moss, R. L. (1989) *J. Gen. Physiol.* **93,** 855–883.
35. Tohtong, R., Yamashita, H., Graham, M., Haeberle, J., Simcox, A. & Maughan, D. (1995) *Nature (London)* **374,** 650–653.